International Journal for Multidisciplinary Research (IJFMR)
E-ISSN: 2582-2160 ● Website: www.ijfmr.com ● Email: editor@ijfmr.com

Biosynthesised Zno Nano-Photo-Catalyst for Degradation of Congo Red Dye for Water Remediation and Study of their Antibacterial and Antifungal Activities

Mrinalini Parmar[1], Brij Bhushan Santosh Pandey[2], Mallika Sanyal[3]

[1]Gujarat Arts and Science College, Ahmedabad, Gujarat, 380009, India
[2,3]St. Xavier's College, Navrangpura, Ahmedabad, Gujarat-380009, India
[1,3]Department of Chemistry, Gujarat University, Ahmedabad, Gujarat-380009, India

Abstract

ZnO Nanoparticles synthesised using *Ricinus cummunis* leaves as reducing and capping agent serves as a good photocatalyst that is utilised to degrade Congo Red Dye which is a common anionic azo dye. The ZnO NPs were confirmed using UV-Vis, IR, XRD and EDX spectroscopy. The size of the nanosized ZnO particles is around 20nm as calculated from images of FE -SEM and HR- TEM. The degradation of Congo Red dye as a function of change in catalyst load and change in dye concentration was studied. The ZnO NPs catalysed degradation was maximum (88%) for 40mg catalyst in 20ppm dye concentration. These particles also exhibit good antibacterial and anti-fungal activities. Antibacterial activities against E.coli and S.aurious were excellent whereas antifungal activities against *Candida albicans* was better than *Aspergillus fumigatus.* The IC $_{50}$ value for *Candida albicans was 132*.

Keywords: Photocatalyst, Congo Red Dye Degradation, Antifungal, Antibacterial

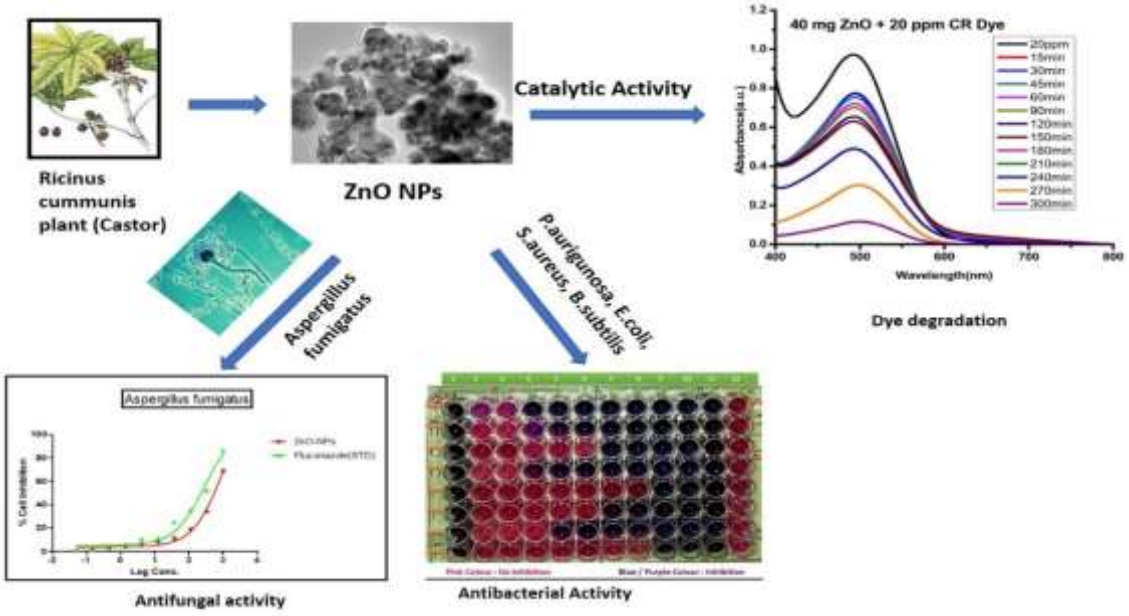

1. Introduction

Nanotechnology has been tremendously escalating branch of material science that is researched over the past few years. The difference in properties of nanomaterial from its parent bulk material makes them uniquely interesting. Nanoparticles owe these distinct properties to their high tensile strength, large surface to volume ratio and a greater number of active sites on the surface area (Fouladi-Fard et al., 2022). These properties make them highly desirable to be used in pharmaceutics, bio medics, cosmetics, water treatment and optics (Mata et al., 2016). Preparation of Nanoparticles can be achieved using many methods like laser ablation, chemical vapour deposition, sol gel, microwave, deposition- precipitation, microbes and green biomass (Ping et al., 2018). Most of these methods require either cumbersome experimental conditions or utilise toxic chemicals for synthesis process. Among these environmentally benign methods include preparation of metal nanoparticles and their composites using biomass and microorganisms. They do not produce any toxic by-products and their method of preparation is also less cumbersome and more economic. Nanomaterials thus, prepared using plant biomass is of great interest. One pot green synthesis of nanomaterials can be achieved by utilising the reducing and stabilising potential of the compounds present in the plants. The biosynthesis of nanomaterials through this path is sustainable, hazard free and economic. It is also easier to prepare desired nanomaterials by this process as it does not require any complicated and cumbersome setup and conditions (Parmar & Sanyal, 2022))Click or tap here to enter text.Plants capture approximately 75% of the solar energy and convert them into chemical energy, hence plants serve as a good candidate for synthesising nanoparticles in an economic and easy pathway (Noohpisheh et al., 2020)

Metal oxide nano particles are widely been researched in recent times. Among them ZnO nanoparticles are unique as they possess semiconducting, pyro, piezo and optical properties and are biodegradable nanoparticles. They are considered to be of n-type semiconductor with a large band gap (MuthuKathija et al., 2023)(Marambio-Jones & Hoek, 2010). Lately ZnO has been used in sunscreens, ointments, self-cleaning glasses and bio medics. They prove to have great potential as antibacterial, antifungal as well as anticancer agent. They also find usage in water remediation because of their catalytic properties (C. et al., 2016).They act as photocatalyst and play a vital role in degradation of toxic dyes present in water bodies. Other physical and physicochemical methods like coagulation, flocculation, adsorption and reverse osmosis techniques remove the colour of the water but removal of residual compound (colourless) which is even more toxic remains persistent. The degradation of dyes by photosensitive materials can lead to their conversion into carbon dioxide, water and some inorganic ions which are benign to the environment. Congo red is a common anionic azo dye which is commonly used in textile, paper and rubber industries (Ganapuram et al., 2015).The toxic Dye is removed photo catalytically when an electron hole pair is created on the surface of the catalyst. When incident radiation with wavelength more than the band gap of the catalyst falls on a photocatalyst it produces hydroxide radical, superoxide anion radical which eventually reacts with dye molecules to produce environmentally benign compounds (Parmar & Sanyal, 2022, (Nierman et al., 2005)

2. Materials and Methods

2.1 Materials

Fresh leaves of *Ricinus cummunis* were collected from a local farm. $Zn(NO_3)_2.6H2O$ (CAS no.- 10196-18-6) and Congo Red Dye were purchased from SRL laboratories, Maharashtra, India. All chemicals were of analytical grade and used without further purification. Double distilled water was used for carrying out

all the experiments.

2.2 Methodology

2.2.1 Preparation of ZnO Nanoparticles

We have prepared ZnO Nanoparticles using dry leaves extract of *Ricinus Cummunis* with slight modifications in the method applied by Chennimalai et al.(Chennimalai et al., 2019) Freshly collected leaves of *Ricinus cummunis* were washed in double distilled water twice and allowed to dry in shade for 10 days. The dry leaves were then weighed and about 20gms of leaves were crushed to powder in a grinder and added to 80 ml of water. The mixture was stirred at 500 rpm at 80 deg. for 30 mins. until a yellow-coloured precipitate is obtained. The precipitate is dried in oven for 8-10 hrs at 80 degree and then calcined at 400 degrees in a muffle furnace 2 hours. The final product is a white coloured amorphous powder. The Nanoparticles thus obtained were stored in an air tight container for further use.

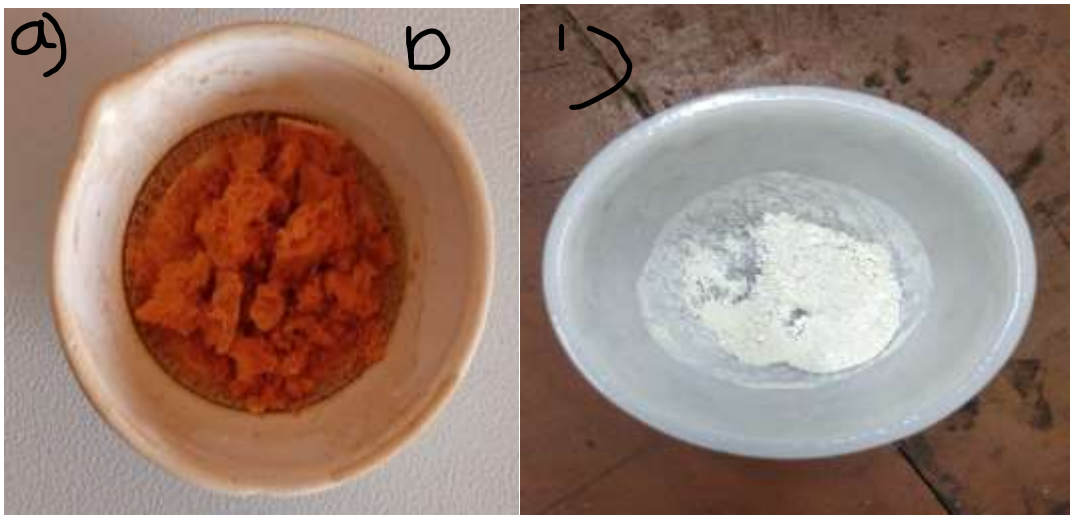

Figure 1: a) Precipitate of ZnO after drying in oven b) ZnO NPs after calcination at 400 degrees

2.2.2 Characterisation of ZnO Nanoparticles

The preliminary confirmation of prepared Nanoparticles was done using UV spectrophotometer (UV-1800 Shimadzu). The range was between wavelength 200nm-800 nm with scanning speed of 1nm/sec. FT-IR spectroscopy was done using Shimadzu Make FTIR (Model IR Affinity-1S) between range 400cm^{-1} - 2000cm^{-1}. XRD data was analysed using a X-Ray Diffractometer (Rigaku, Miniflex-600 Tokyo, Japan) having a scanning speed of 10 deg./min, Cu-K radiation (λ= 1.542) detector and graphite monochromator. To acquire data the sample (ZnO NPs) was scanned with continuous scan mode through 2 Θ range of 30-900. HR-TEM was conducted using Jeol, model 2100 plus, Japan operated at 200kv. For FE-SEM the Nova Nano FEG-SEM 450 was used with a resolution of 1nm at 15 kV.

2.2.3. Catalytic Degradation

For catalytic degradation studies, a series of experiments were carried out to analyse the effect of dye concentration and catalyst load. 20 ml of 10 ppm, 20ppm and 30ppm Congo Red dye solutions were mixed with 30mg ZnO Nanoparticle to study the effect of dye concentration. The solution was stirred at 500 rpm in dark conditions to achieve equilibrium and then kept in UV chamber. About 3 ml of solution is taken in a quartz cuvette and UV spectra is analysed for the same at regular intervals. In a similar process for studying the effect of catalyst load 20mg, 30mg and 40mg of ZnO nanoparticles were mixed with 20 ml

20ppm and studied under UV spectrophotometer. The decrease in characteristic peaks of Congo Red dye depicts the degradation process. The percentage degradation can be calculated using formula:

$\frac{A0-A}{A0}$ =% Degradation

Where A0 is the absorbance at time t=0 and A=Absorbance at different time intervals.

2.2.4 Antibacterial Studies

Preparation of sample:

Test compound was prepared using 1:2 dilution method according to the concentration given in Table -1. Well No. 10 contains 1000µg/ml test compound and on serial dilution, a final dilution of test compound is 1.95 µg/ml.

Well no. 1 – 9 contain complete media										
Well no.	1	2	3	4	5	6	7	8	9	10
Sample dilution	50 µl from well 2	50 µl from well 3	50 µl from well 4	50 µl from well 5	50 µl from well 6	50 µl from well 7	50 µl from well 8	50 µl from well 9	50 µl from well 10	150 µl T.S.
Final conc. (µm)	1.95 µg/ml	3.91 µg/ml	7.81 µg/ml	15.62 µg/ml	31.25 µg/ml	62.5 µg/ml	125 µg/ml	250 µg/ml	500 µg/ml	1000 µg/ml

Table 1-1:2 dilution method for preparation of test compound

***Preparation of plates*:**

Microdilution susceptibility testing was performed in flat- bottom 96-well clear plates containing broth medium (50µl) in each well. Sample solutions (50µl) were subsequently serially diluted two-fold in the plates with the broth, starting with the final concentration of 500 mg/L. The working inoculum suspension (50µl) was added to give a final inoculum concentration of 0.5–2.5*10^3 CFU/ml. Ofloxacin was used as the standard antibacterial drug. Sterility and growth controls in the presence of DMSO were also included. The plates were then incubated at 37°C for 24h. After 24 hours resazurin (30µl) is added to each well and incubated for 30 min. MIC was determined through recording the colour change observed.

2.2.5 Antifungal Studies

Antifungal tests were done using standard method of NCCLS (National committee for clinical laboratory standards). 1:3 dilution method was followed for dilution of test compounds and reference (table-2). Fluconazole was considered as standard drug for antifungal activity.

***Preparation of plates*:**

Microdilution susceptibility testing was performed in flat bottom 96-well clear plates containing broth medium (50µl) in each well. Sample solutions (50µl) were subsequently serially diluted two-fold in the plates with the broth, starting with the final concentration of 5000 mg/L. The working inoculum suspension (50µl) was added to give a final inoculum concentration of 0.5–2.5 * 10^3CFU/ml. Sterility and growth controls in the presence of DMSO were also included. The plates were then incubated at 37 °C for 48 h. The amount of growth was measured using plate reader at λ=492nm, [NCCLS document M27-A2](Palanichamy' & Nagarajanb, 1990)(Kaplan et al., 1977)

Well no. 1 – 9 contain complete media 100 µl										
Well no.	1	2	3	4	5	6	7	8	9	10
Sample dilution	50 µl from well 2	50 µl from well 3	50 µl from well 4	50 µl from well 5	50 µl from well 6	50 µl from well 7	50 µl from well 8	50 µl from well 9	50 µl from well 10	150 µl T.S.
Final conc. (µm)	0.050 µg/ml	0.15 µg/ml	0.45 µg/ml	1.37 µg/ml	4.11 µg/ml	12.34 µg/ml	37.03 µg/ml	111.1 µg/ml	333.33 µg/ml	1000 µg/ml

Table No 2: 1:3 dilution of test compound used in the assay

3. Results and Discussion

3.1 Biosynthesis of ZnO Nanoparticles

ZnO Nanoparticles were synthesised using dry leaves of *Ricinus cummunis* plant with slight modifications in the method used by Chennimalai et. al.(Chennimalai et al., 2019).The prepared Nanoparticles were confirmed using UV Spectroscopy, X-Ray Diffraction Spectra, IR Spectra, HR TEM and FE SEM.

UV Visible Spectroscopy

The Nanosized ZnO particles were primarily detected visually by their white colour and then confirmed by UV Spectra. The typical peak for ZnO is at around 382 nm (Azizi et al., 2016).The Direct band gap for ZnO NPs was estimated from a plot between $(\alpha h\boldsymbol{\upsilon})^2$ vs $h\boldsymbol{\nu}$ by extrapolating the linear portion of the curve to the energy axis. The Tauc's formula relating absorption coefficient and photon energy is**:** $\boldsymbol{\alpha E=\alpha_0(E-E_g)^n}$ where α is absorption coefficient, $\boldsymbol{\alpha_0}$ is constant and E is energy of incident photon. n=2 for direct and n=1/2 is considered for indirect band gap. The direct band gap energy is 2.15 eV which is close to the band gap value reported by Lad et.al. The reduction in Band Gap of semiconductors is generally attributed to doping or fast crystallisation process like usage of microwave irradiation but decrease from standard value for undoped material like in our case can be explained due to presence of Oxygen defects. These defects may cause a change in lattice parameters leading to a lower Band gap energy(Lad et al., 2023) .

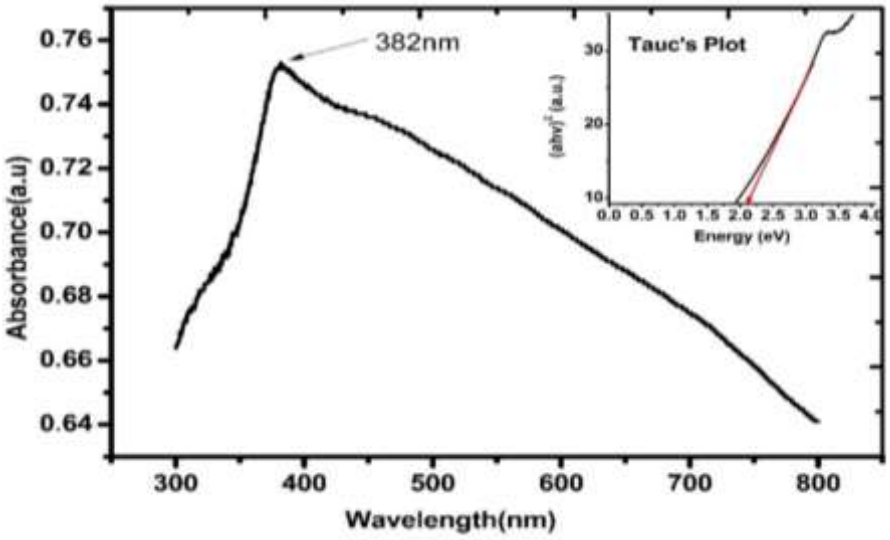

Figure 2(a)-UV visible spectrum of ZnO NPs (b) Band Gap in ZnO NPs (inset)

XRD

The X- Ray Diffraction data reveals the peaks at 2Θ = 31.8 degree, 34.48 degree, 36.28 degree, 47.58 degree and 56.6 degree,62.8 degree and 68.04 degree corresponding to the miller indices (100), (002), (101), (102), (110), (103) and (112) respectively. . The XRD pattern reveals a typical pattern for pure ZnO NP (Gawade et al., 2017). The average size determined using Scherrer's equation.

$D=k\lambda/(\beta \cos\theta)$ -----(i)

was found to be 57.5 nm, where, D is the average size of the nanoparticles, k is geometric factor (0.9), λ is the wavelength of X-ray radiation source and b is the angular FWHM (full-width at half maximum) of the XRD peak at the diffraction angle θ.

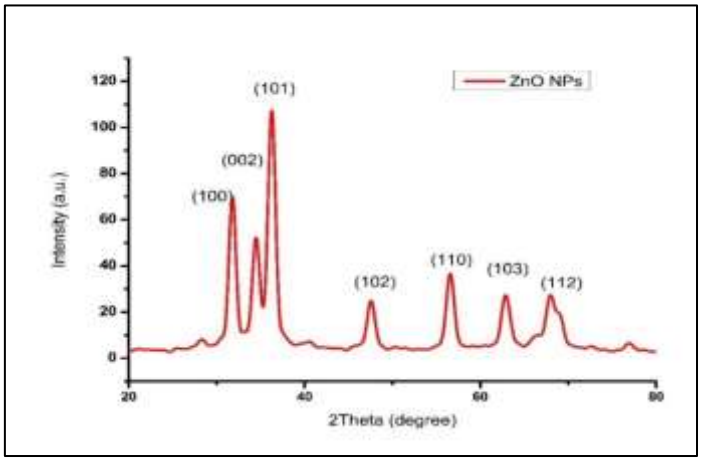

Figure-3 XRD pattern of ZnO NPs

TEM and EDX

The shape of the prepared ZnO NPs is mostly found to be spherical along with some hexagonal particles, when analysed using High Resolution Transmission Electron Microscope (HR-TEM). The size distribution chart reveals that maximum number of particles have size between 20-25 nm. The average size being 28.38 nm. elemental nature of the prepared ZnO NPs was confirmed by EDX. Signal for Copper is probably due to the carbon supported copper grid used for sample preparation. The weight percentage being 75.21% for Zinc and 24.79% for Oxygen.

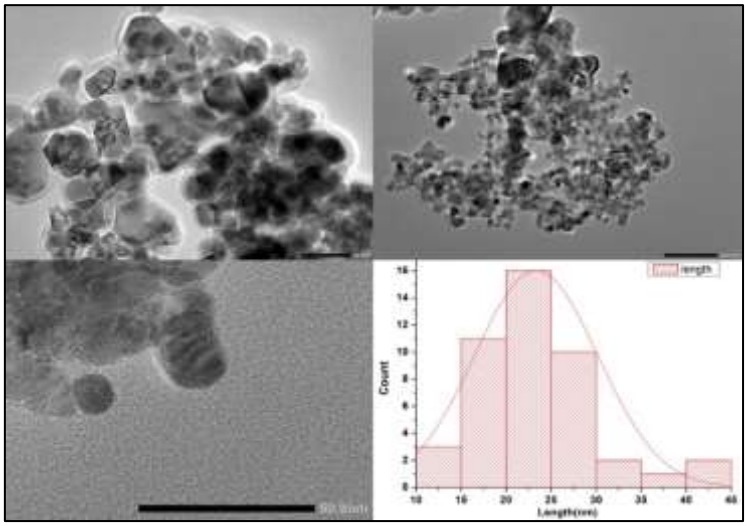

Figure-4: HR-TEM images and histogram revealing size distribution of ZnO NPs

FE-SEM

The morphology of ZnO NPs as evident from FE SEM is spherical shape. There is agglomeration of ZnO NPs which is clearly visible in the data achieved from SEM images. Most of the particles are having size between 15nm -25nm, the Average size being 20.65nm. The data is close to size calculated by TEM.

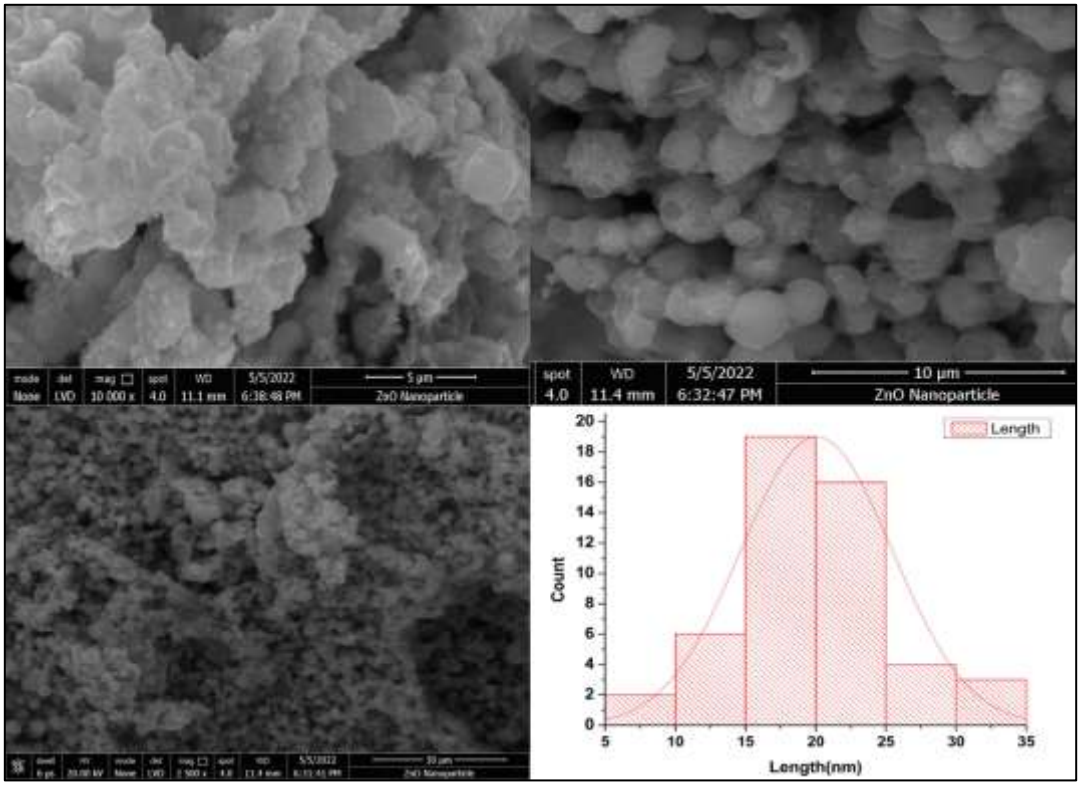

Figure-5: FE SEM images and histogram revealing size distribution of ZnO NPs

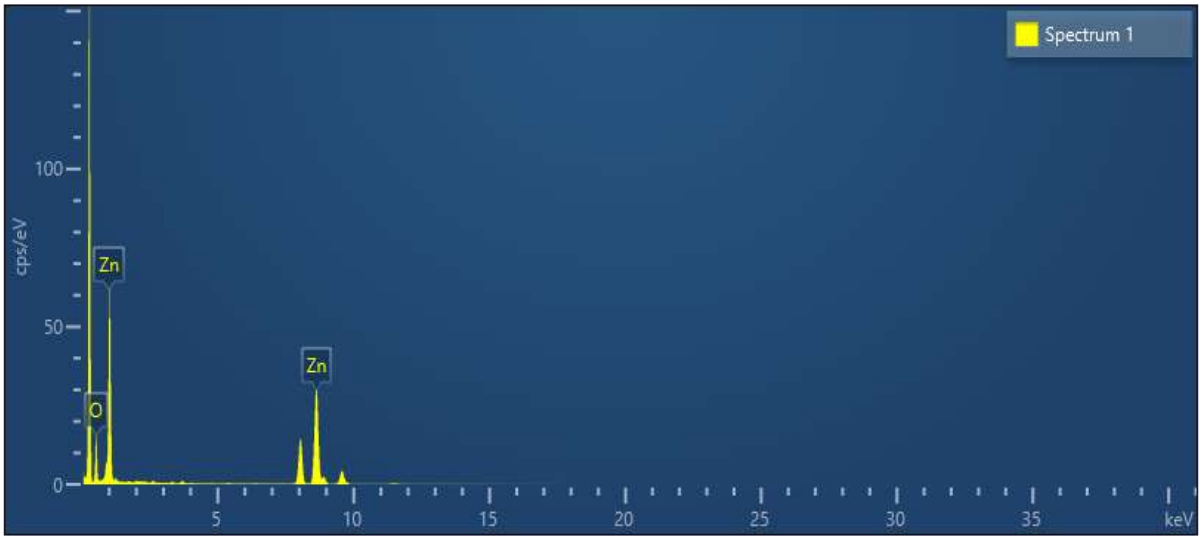

Figure-6: EDX Spectra of ZnO NPs

InfraRed Spectra

The spectrum shows bands at 3346cm^{-1} for presence of OH stretching frequency of polyphenols (Jamdagni et al., 2018). 2369cm^{-1} depicts enol of diketone. Peaks corresponding to 1470cm^{-1} is majorly due to

presence of C=C or N-H bending vibrations (Król et al., 2019). 1136cm-1 is attributed to C-N stretching vibrations of aliphatic, aromatic amides and amines and sharp peak at 916 is due to C=C-H of alkynes (Bhuyan et al., 2015).

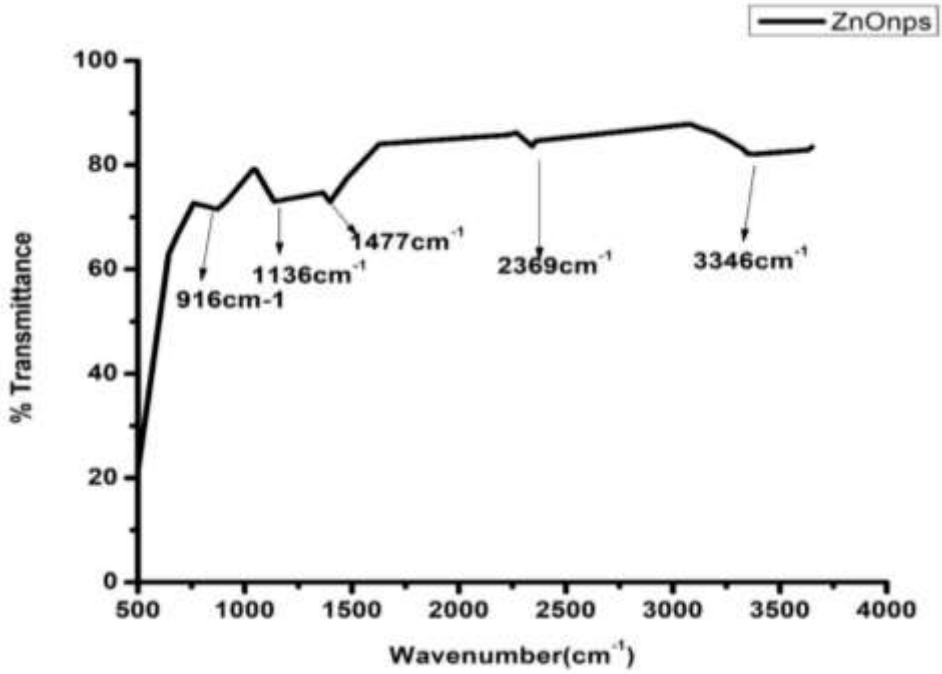

Figure 7- IR Spectra of ZnO NPs

3.2 Catalytic degradation of Congo Red Dye

Catalytic degradation aspect of the synthesised ZnO NPs was studied on Congo Red Dye (CR). CR dye is a red coloured azo dye which has N=N linkage. The reduced form of this dye is colourless. CR is widely used in paper, rubber, plastic and textile industries. It is an anionic azo dye with absorption maxima at 498 nm ($\pi \rightarrow \pi^*$) and 350nm ($n \rightarrow \pi^*$) (Ganapuram et al., 2015). The degradation is due to the excitation of a valence electron from the valence band to the conduction band of the metal nanomaterial on exposure of UV radiation. This process leads to the formation of hole in conduction band and electron pair in the valence band if the gap between the two bands is less than the incident radiation. The excited electron which has migrated to the surface of the catalyst is responsible for reacting with molecules in close proximity with oxygen molecule to give superoxide ion radical (Rauf & Ashraf, 2009) (Ganapuram et al., 2015.

Catalyst + $\mathbf{h\nu} \rightarrow e^-_{cb} + h^+_{vb}$ -----(i)

$H_2O + h^+_{vb} \rightarrow OH^\cdot + H^+$ -----(ii)

$O_2 + e^-_{cb} \rightarrow O^-_2$. -----(iii)

$OH^\cdot + O^-_2$ + Dye molecules → Degradation products (CO_2, H_2O) -----(iv (Ganapuram et al., 2015)

Variation of catalyst load

On changing amount of catalyst from 20mg to 40mg at constant dye concentration of 20 ppm at pH=7, it is observed that the rate of degradation increases from 72.3% to 88.2%.The possible reason may be increase in surface area for degradation process with increase in catalyst concentration. The reaction is of first order with rate constants varying between 0.0038 min^{-1} and 0.0081 min^{-1} for 40mg ZnO Nano catalyst in 20ppm CR dye solution and 20mg ZnO Nano catalyst in 20ppm CR dye solution respectively.

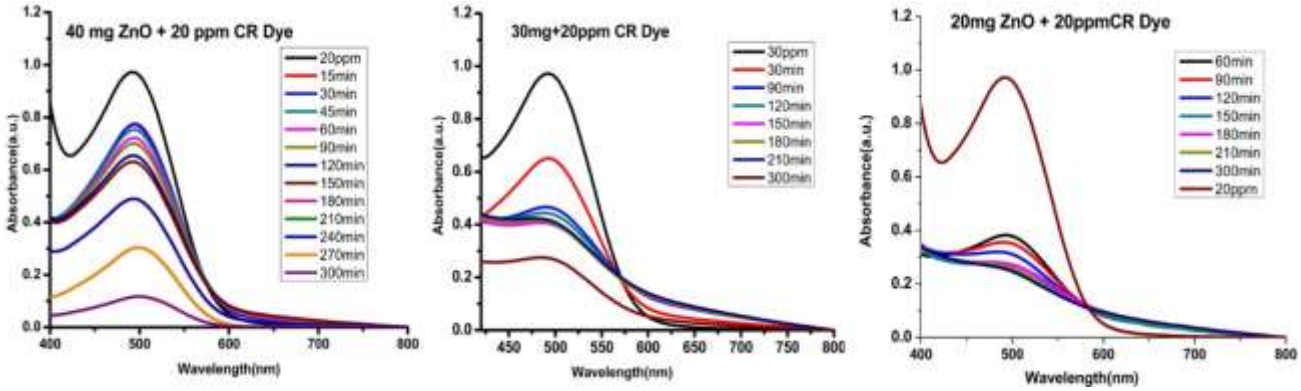

Figure 8- Decrease in absorbance maxima of Congo Red dye with decrease in Catalyst load.

Variation of dye Concentration

On changing concentration of Dye from 10ppm to 30ppm at constant ZnO Nano catalyst of 30mg at pH=7,it is observed that the rate of degradation decreases from 84.69% to 72.4 % respectively for a constant time period of 5hours. On increasing dye concentration at constant catalyst load, the effective surface for degradation remains same but dye molecules increases per unit volume leading to a decrease in degradation percentage. The results are in accordance with the degradation studies using green synthesised Au and Ag nanoparticles. (Parmar et al., 2023b; Parmar & Sanyal, 2024)

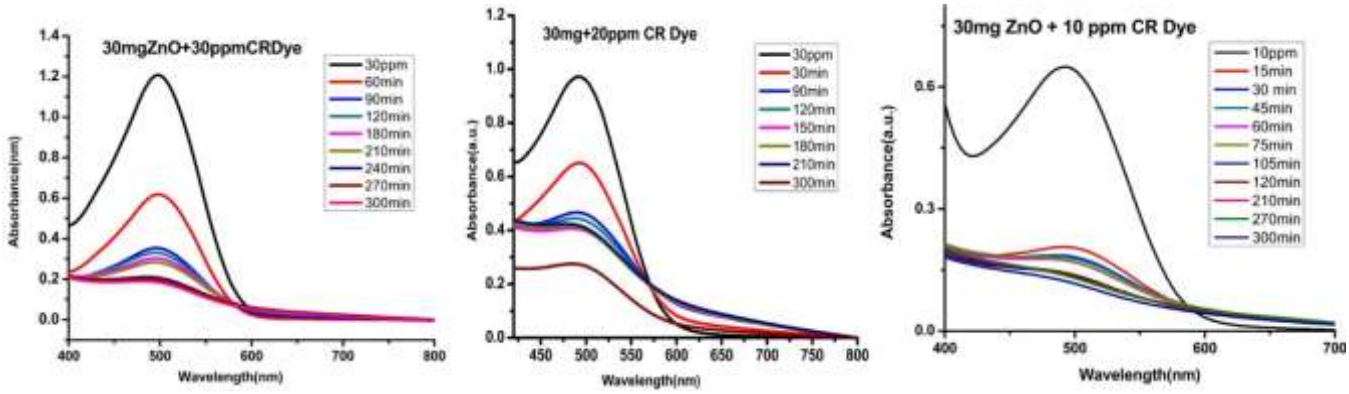

3.3 Antibacterial Activity

The antibacterial activity is determined by observing the change in colour of the plate containing bacterial culture on addition of Resazurin. The change of colour from blue to pink indicates MIC (Minimum Inhibitory Concentration). Blue colour of Resazurin confirms viable organism while the pink colour indicates inhibition of growth of micro-organism. The efficacy of the ZnO NPs is determined by comparing results with standard drug Streptomycin.

Sample	**Row**	**1**	**2**	**3**	**4**	**5**	**6**	**7**	**8**	**9**	**10**	**Bacteria**
	µg/ml	**1.95**	**3.90**	**7.81**	**15.625**	**31.250**	**62.5**	**125**	**250**	**500**	**1000**	
	A	-	+	++	+++	+++	+++	+++	+++	+++	+++	***E.coli***
	B	-	-	+	+	++	+++	+++	+++	+++	+++	***E.coli***
ZnO NPs	C	-	-	-	-	+	++	+++	+++	+++	+++	***B.subtilis***

	F	-	-	-	-	-	+	++	+++	+++	+++	***B.subtilis***
	D	-	+	++	+++	+++	+++	+++	+++	+++	+++	***S.aurious***
	G	-	-	+	+ +	+++	+++	+++	+++	+++	+++	***S.aurious***
	E	-	-	-	-	-	-	+	++	++	+++	***P.aeruginosa***
	H	-	-	-	-	-	-	-	+	++	+++	***P.aerigunosa***
Streptomycin		-	-	-	-	-	+	++	+++	+++	+++	***P.aurigunosa***
		-	-	-	-	-	-	-	-	+	++	***S. aureus***
		-	-	-	-	-	-	+	++	+++	+++	***B.subtilis***
		-	+	++	+++	+++	+++	+++	+++	+++	+++	***E.coli***
- **No Inhibition (growth found)** + **Minimum Inhibitory Concentration**												

Table 3- Antibacterial study on *E.coli, B.subtilis, S.aurious and P. aurigunosa* bacterial strains.

ZnO NPs provide excellent activity on E.coli and S.aurious bacterial strains, the average MIC being 5.86 µg/ml. ZnO shows better activity on these strain when compared to standard drug streptomycin. Medium activity is observed for B. subtilis whereas least activity is observed for P.aurigunosa, average MIC being 187.5 µg/ml .

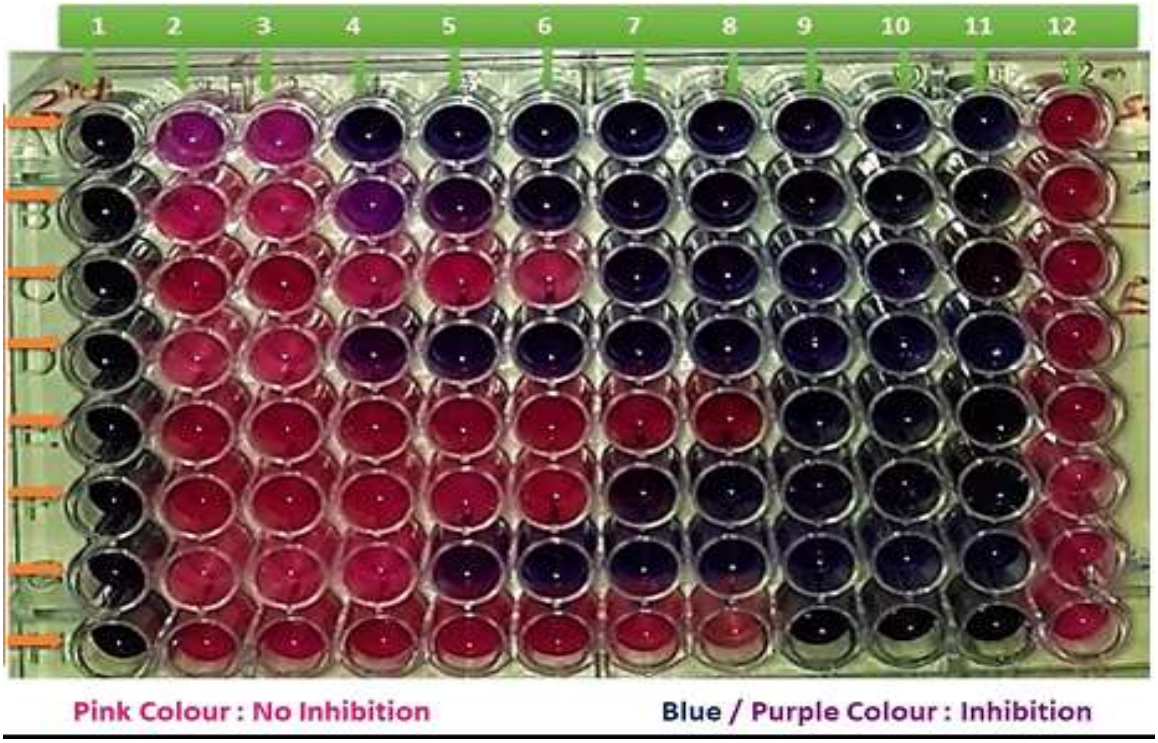

Figure 10- Microbroth dilution technique for testing ZnO NPs as test sample against *E.coli, B.subtilis, S.aurious and P. aurigunosa* bacterial strains

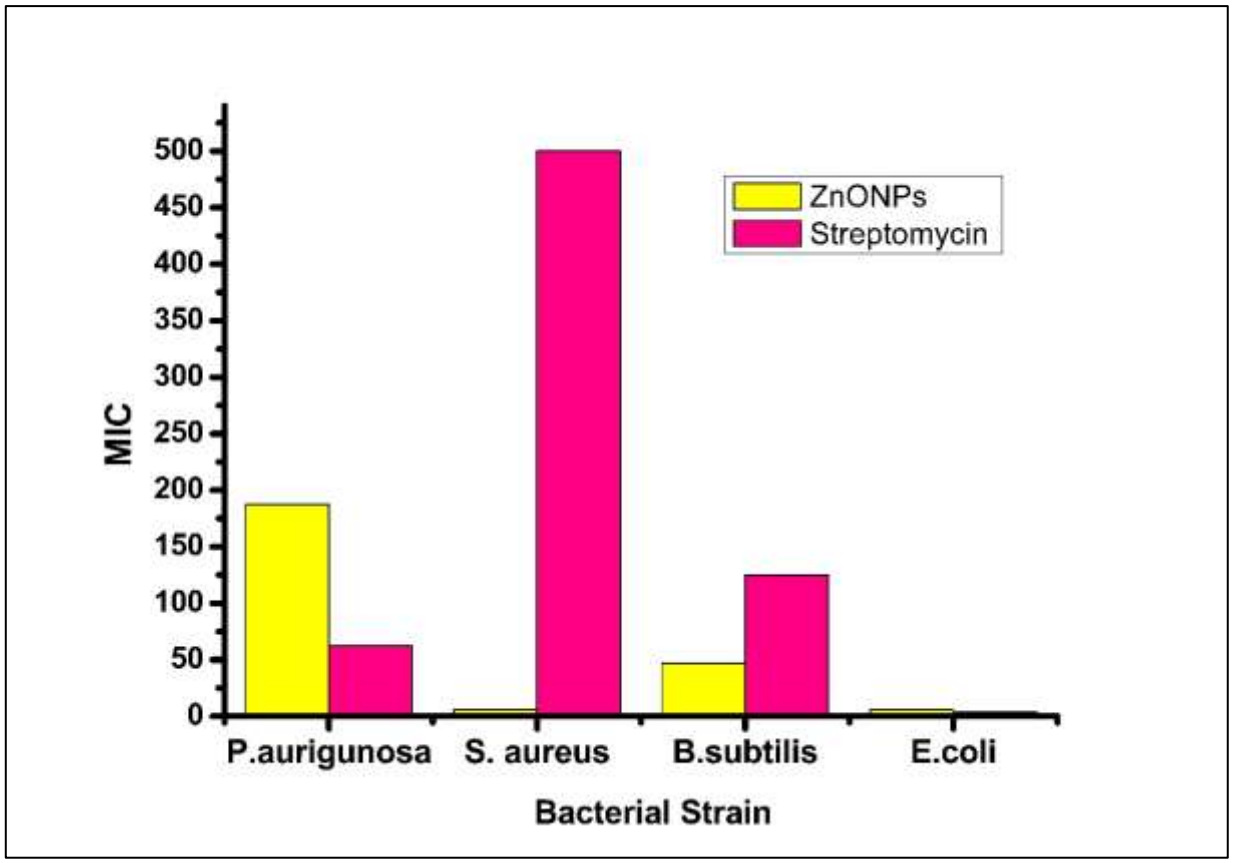

Figure11 Comparative study of effect of ZnO NPs as Antibacterial agent against Steptomycin.

3.4 Antifungal Study

Candida albicans and *Aspergillus fumigatus* are the fungal strains used for the present study. *Candida albicans* is the most commonly isolated yeast causing diseases in humans. Candidiasis, is a common yeast infection that includes vaginitis, oral thrush and potentially life threatening diseases. Members of the Aspergillus genus are largely responsible for a large spectrum of diseases called Aspergillosis. The rate of infection in immunocompromised individuals is around 50% and rate of mortality can often rise 50%.(Al-Tawfiq & Wools, n.d.; Esterre et al., 1996)

Fluconazole and ZnO NPs were tested against *Candida albicans* and *Aspergillus fumigatus* in dose dependent manner. ELISA plate reader was used to determine end point spectrophotometrically. NCCLS test replicates for anti-fungal activity were analysed every 24 hr for two days to determine the percentage growth inhibition in the presence of the drug and ZnO NPs solution.

Tested compounds were serially diluted in concentration range of 1000 to 1.95 µg/ml in plates with the fungal strain. The working inoculums suspension were added to give final inoculums concentration of 0.5–2.5 X 10^3CFU/ml. The plates were incubated at 37°C for 48 h. The amount of growth was measured using plate reader at λ=450nm. Data were analysed using Graph pad Prism with use of Dose response curve equation. Data were normalized and curve fitting was opted with 95% confidence limit. IC50 was derived from curve of % Inhibition V/s Log dose of compound. This assay was also performed for Amphotericin B.

Percentage inhibition of the extract against all cell line was calculated using the following formula.

% cell survival = (AT-AB) / (AC-AB) X 100

Where,

AT=Absorbance of treated cells (drug)
AB=Absorbance of blank (without cell)
AC=Absorbance of control (untreated)
There by,
% Cell growth inhibition= = 100 - Percentage cell survival
The activity report of our test compound against *candida albicans* and *aspergillus fumigatus* is determined using IC_{50} value and R^2 values obtained from log concentration vs % cell inhibition. The ZnO NPs shows IC50 value of 132.5 µg/ml against *candida albicans* and IC50 value of *941.5* µg/ml against *aspergillus fumigatus*. The test compound shows higher activity against candida albicans in comparison to aspergillus fumigatus. The linearity for aspergillus fumigatus is also higher than that of candida albicans.

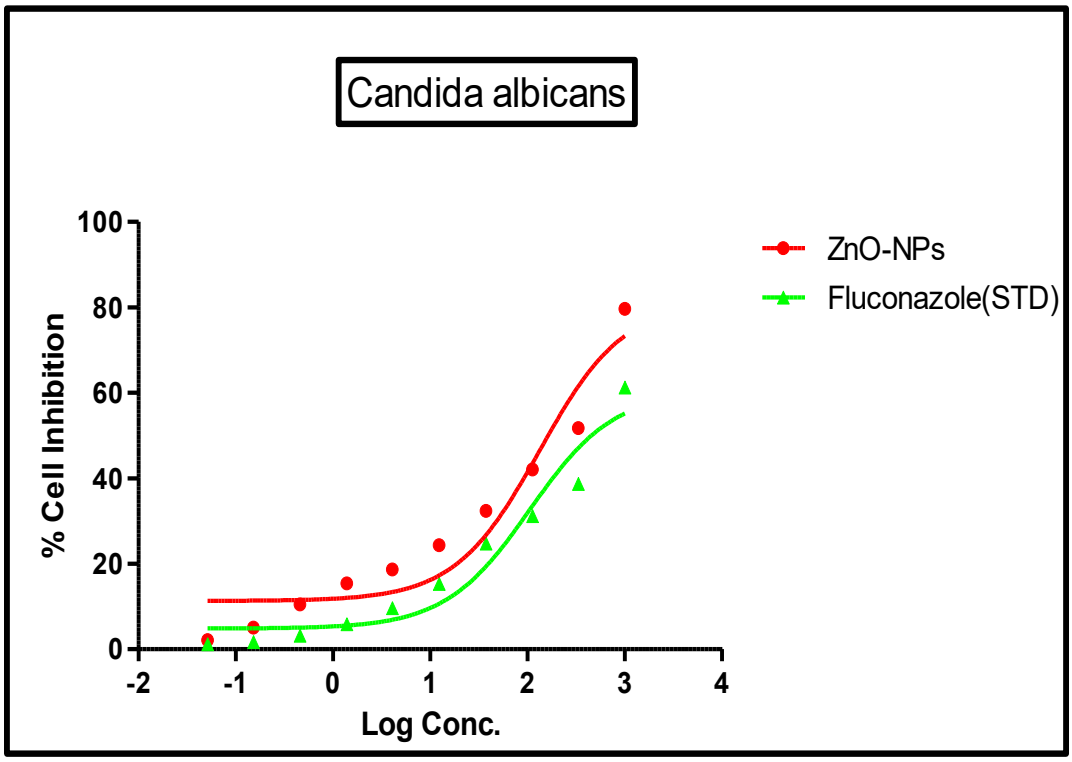

Figure 12 Dose response curve of Test compounds and Fluconazole against *Candida albicans*

Conc (µg/ml)	Log Conc.	ZnONPs	Fluconazole(STD)
0.05	-1.29	2.130	-0.65
0.15	-0.82	5.032	0.95
0.46	-0.34	10.52	1.365
1.37	0.14	15.42	3.062
4.12	0.61	18.64	5.081
12.35	1.09	24.32	11.24
37.04	1.57	32.34	18.97
111.11	2.05	42.08	35.82
333.33	2.52	51.74	61.05
1000	3.00	79.68	65.31

IC_{50} µg/ml	**132.5**	**108.3**
R^2	**0.9264**	**0.9920**

Table 4-Percentage growth inhibition by test compounds against *Candida albican* strain and Fluconazole (Std.)

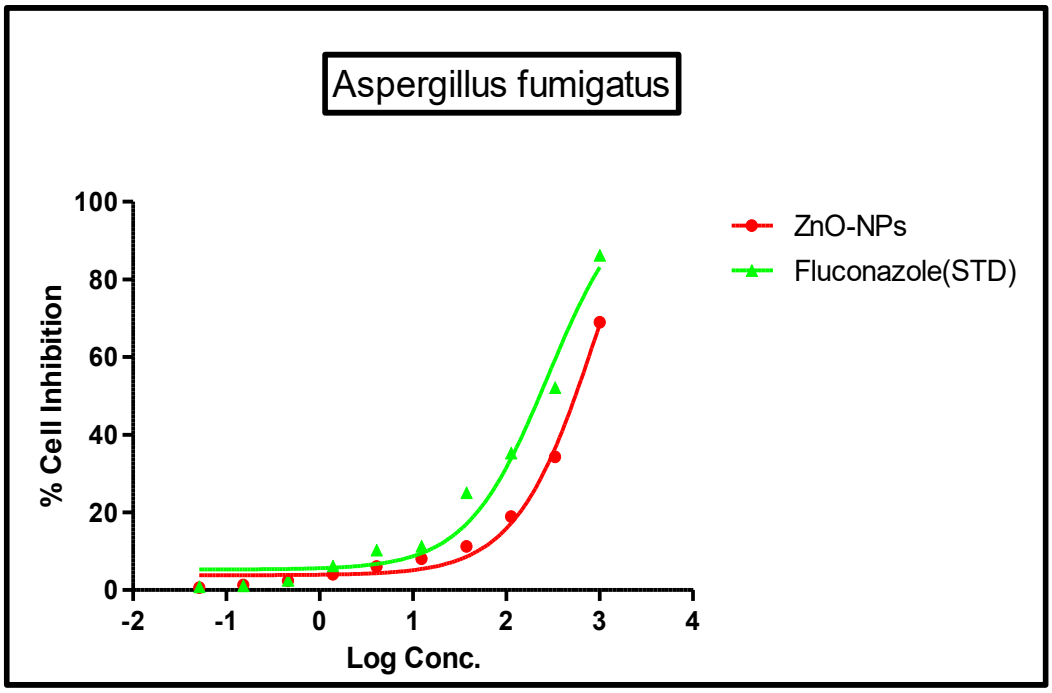

Figure 13- Dose response curve of Test compounds and Fluconazole against *Aspergillus fumigatus*.

Conc (µg/ml)	**Log Conc.**	**ZnONPs**	**Fluconazole(STD)**
0.05	-1.29	0.652	0.85
0.15	-0.82	1.325	1.15
0.46	-0.34	2.352	2.547
1.37	0.14	4.052	6.245
4.12	0.61	6.032	10.35
12.35	1.09	8.085	11.35
37.04	1.57	11.23	25.13
111.11	2.05	18.962	35.26
333.33	2.52	34.26	52.16
1000	3.00	68.95	86.23
IC_{50} µg/ml		**941.5**	**278.7**
R^2		**0.9893**	**0.9725**

Table 5- Percentage growth inhibition by test compounds against *Aspergillus fumigatus* strain and Fluconazole (Std.)

Conclusion

It can be concluded from this study of synthesis of ZnO nanoparticles utilising leaf extract of Ricinus cumminis that it serves as a good catalyst for degradation of Congo Red dye. On increasing catalyst load the rate of degradation increases to approximately 88% whereas on increasing dye concentration at constant catalyst load the degradation process increases to 85%. Apart from being a goog photocatalyst they also exhibit antibacterial and antifungal properties. ZnO NPs provide excellent activity on E.coli and S.aurious bacterial strains as compared to standard drug streptomycin. The average MIC being 5.86 µg/ml. The ZnO NPs provide good antifungal properties against *candida albicans*. The value of IC50 being 132.5 when compared with standard drug Flucanozone.

Ethical Statement

This article does not contain any studies involving animals or human performed by any of the authors.

Conflict of Interest

The authors declare that they have no known competing financial interests or personal relationships that could have appeared to influence the work reported in this paper.

Funding

No funding has been received for performing this research work.

Acknowledgement

We are thankful to Punjab university for HR TEM analysis of the sample. We also thank Dr Vipul Patel, Sanjivani College of Pharm Education, Kopargaon, Maharashtra for his assistance in antifungal studies.

Data Availability

“The data that support the findings of this study are available with the corresponding author upon reasonable request."

References

1. Al-Tawfiq, J. A., & Wools, K. K. (n.d.). *Disseminated Sporotrichosis and Sporothrix schenckii Fungemia as the Initial Presentation of Human Immunodeficiency Virus Infection*. http://cid.oxfordjournals.org/
2. Arya, G., Sharma, N., Ahmed, J., Gupta, N., Kumar, A., Chandra, R., & Nimesh, S. (2017). Degradation of anthropogenic pollutant and organic dyes by biosynthesized silver nano-catalyst from Cicer arietinum leaves. *Journal of Photochemistry and Photobiology B: Biology*, *174*, 90–96. https://doi.org/10.1016/j.jphotobiol.2017.07.019
3. Azizi, S., Mohamad, R., Bahadoran, A., Bayat, S., Rahim, R. A., Ariff, A., & Saad, W. Z. (2016). Effect of annealing temperature on antimicrobial and structural properties of bio-synthesized zinc oxide nanoparticles using flower extract of Anchusa italica. *Journal of Photochemistry and Photobiology B: Biology*, *161*, 441–449. https://doi.org/10.1016/j.jphotobiol.2016.06.007
4. Bhuyan, T., Mishra, K., Khanuja, M., Prasad, R., & Varma, A. (2015). Biosynthesis of zinc oxide nanoparticles from Azadirachta indica for antibacterial and photocatalytic applications. *Materials Science in Semiconductor Processing*, *32*, 55–61. https://doi.org/10.1016/j.mssp.2014.12.053

5. C., V., Prabha, M. N. C., & Raj, M. A. L. A. (2016). Green mediated synthesis of zinc oxide nanoparticles for the photocatalytic degradation of Rose Bengal dye. *Environmental Nanotechnology, Monitoring and Management*, *6*, 134–138. https://doi.org/10.1016/j.enmm.2016.09.004
6. Chennimalai, M., Do, J. Y., Kang, M., & Senthil, T. S. (2019). A facile green approach of ZnO NRs synthesized via Ricinus communis L. leaf extract for Biological activities. *Materials Science and Engineering C*, *103*. https://doi.org/10.1016/j.msec.2019.109844
7. Esterre, P., Inzan, C. K., Ramarcel, E. R., Andriantsimahavandy, A., Ratsioharana, M., Pecarrere, J. L., & Roig, P. (1996). SESSION III Treatment of chromomycosis with terbinafine: preliminary results of an open pilot study. In *British Journal of Dermatology*.
8. Fouladi-Fard, R., Aali, R., Mohammadi-Aghdam, S., & Mortazavi-derazkola, S. (2022). The surface modification of spherical ZnO with Ag nanoparticles: A novel agent, biogenic synthesis, catalytic and antibacterial activities. *Arabian Journal of Chemistry*, *15*(3). https://doi.org/10.1016/j.arabjc.2021.103658
9. Ganapuram, B. R., Alle, M., Dadigala, R., Dasari, A., Maragoni, V., & Guttena, V. (2015). Catalytic reduction of methylene blue and Congo red dyes using green synthesized gold nanoparticles capped by salmalia malabarica gum. *International Nano Letters*, *5*(4), 215–222. https://doi.org/10.1007/s40089-015-0158-3
10. Gawade, V. V., Gavade, N. L., Shinde, H. M., Babar, S. B., Kadam, A. N., & Garadkar, K. M. (2017). Green synthesis of ZnO nanoparticles by using Calotropis procera leaves for the photodegradation of methyl orange. *Journal of Materials Science: Materials in Electronics*, *28*(18), 14033–14039. https://doi.org/10.1007/s10854-017-7254-2
11. Jamdagni, P., Khatri, P., & Rana, J. S. (2018). Green synthesis of zinc oxide nanoparticles using flower extract of Nyctanthes arbor-tristis and their antifungal activity. *Journal of King Saud University - Science*, *30*(2), 168–175. https://doi.org/10.1016/j.jksus.2016.10.002
12. Kaplan, M. H., Rosen, P. P., & Armstrong, D. (n.d.). *CRYPTOCOCCOSIS IN A CANCER HOSPITAL Clinical and Pathological Correlates in Forty-Six Patients*.
13. Król, A., Railean-Plugaru, V., Pomastowski, P., & Buszewski, B. (2019). Phytochemical investigation of Medicago sativa L. extract and its potential as a safe source for the synthesis of ZnO nanoparticles: The proposed mechanism of formation and antimicrobial activity. *Phytochemistry Letters*, *31*, 170–180. https://doi.org/10.1016/j.phytol.2019.04.009
14. Lad, P., Pathak, V., Thakkar, A. B., Thakor, P., Deshpande, M. P., & Pandya, S. (2023). ZnO Nanoparticles Synthesized by Precipitation Method for Solar-Driven Photodegradation of Methylene Blue Dye and Its Potential as an Anticancer Agent. *Brazilian Journal of Physics*, *53*(3). https://doi.org/10.1007/s13538-023-01278-w
15. Marambio-Jones, C., & Hoek, E. M. V. (2010). A review of the antibacterial effects of silver nanomaterials and potential implications for human health and the environment. In *Journal of Nanoparticle Research* (Vol. 12, Issue 5, pp. 1531–1551). https://doi.org/10.1007/s11051-010-9900-y
16. Mata, R., Bhaskaran, A., & Sadras, S. R. (2016). Green-synthesized gold nanoparticles from Plumeria alba flower extract to augment catalytic degradation of organic dyes and inhibit bacterial growth. *Particuology*, *24*, 78–86. https://doi.org/10.1016/j.partic.2014.12.014
17. MuthuKathija, M., Sheik Muhideen Badhusha, M., & Rama, V. (2023). Green synthesis of zinc oxide nanoparticles using Pisonia Alba leaf extract and its antibacterial activity. *Applied Surface Science*

Advances, *15*. https://doi.org/10.1016/j.apsadv.2023.100400

18. Noohpisheh, Z., Amiri, H., Farhadi, S., & Mohammadi-gholami, A. (2020). Green synthesis of Ag-ZnO nanocomposites using Trigonella foenum-graecum leaf extract and their antibacterial, antifungal, antioxidant and photocatalytic properties. *Spectrochimica Acta - Part A: Molecular and Biomolecular Spectroscopy*, *240*. https://doi.org/10.1016/j.saa.2020.118595
19. Palanichamy', S., & Nagarajanb, S. (1990). *ANTIFUNGAL ACTIVITY OF CASSIA ALATA LEAF EXTRACT*.
20. Parmar, M., Arodiya, F., & Sanyal, M. (2023a). Green Synthesis of Silver Nanoparticles Using Dry Leaf Extract of Ricinus communis and Its Application in Photocatalytic Degradation of Carcinogenic Dyes and Antifungal Studies. *BioNanoScience*. https://doi.org/10.1007/s12668-023-01084-3
21. Parmar, M., Arodiya, F., & Sanyal, M. (2023b). Green Synthesis of Silver Nanoparticles Using Dry Leaf Extract of Ricinus communis and Its Application in Photocatalytic Degradation of Carcinogenic Dyes and Antifungal Studies. *BioNanoScience*, *13*(2), 450–463. https://doi.org/10.1007/s12668-023-01084-3
22. Parmar, M., & Sanyal, M. (2022). Extensive study on plant mediated green synthesis of metal nanoparticles and their application for degradation of cationic and anionic dyes. In *Environmental Nanotechnology, Monitoring and Management* (Vol. 17). Elsevier B.V. https://doi.org/10.1016/j.enmm.2021.100624
23. Parmar, M., & Sanyal, M. (2024). Biosynthesis of gold nanoparticles using aqueous extract of Ricinus cummunis leaves to augment catalytic degradation of organic dyes and study of its antifungal and antibacterial activities. *Particuology*, *87*, 87–98. https://doi.org/10.1016/j.partic.2023.07.018
24. Ping, Y., Zhang, J., Xing, T., Chen, G., Tao, R., & Choo, K. H. (2018). Green synthesis of silver nanoparticles using grape seed extract and their application for reductive catalysis of Direct Orange 26. *Journal of Industrial and Engineering Chemistry*, *58*, 74–79. https://doi.org/10.1016/j.jiec.2017.09.009
25. Rauf, M. A., & Ashraf, S. S. (2009). Fundamental principles and application of heterogeneous photocatalytic degradation of dyes in solution. In *Chemical Engineering Journal* (Vol. 151, Issues 1–3, pp. 10–18). https://doi.org/10.1016/j.cej.2009.02.026